

## Porous MoS<sub>2</sub> Synthesized by Ultrasonic Spray Pyrolysis

Sara E. Skrabalak and Kenneth S. Suslick\*

*School of Chemical Sciences, University of Illinois at Urbana-Champaign, 601 South Goodwin Avenue, Urbana, Illinois 61801*

Received March 15, 2005; E-mail: ksuslick@uiuc.edu

The catalytic removal of oxygen, nitrogen, and sulfur from organic molecules is an important step in petroleum processing.<sup>1</sup> A recent EPA mandate<sup>2</sup> requires a further reduction of such heteroatoms from petroleum, making improved hydrotreating catalysts essential. Specifically, more efficient catalysts for the hydrodesulfurization (HDS) of refractory thiophene-based compounds and residual fuel fractions are urgently needed.<sup>3</sup> To address this, both supported<sup>4</sup> and unsupported<sup>5</sup> catalysts of different chemical compositions have been prepared by a variety of synthetic techniques. Here, ultrasonic spray pyrolysis<sup>6</sup> (USP) has been used to synthesize porous, nanostructured MoS<sub>2</sub>, a typical HDS material. Unless modified,<sup>7</sup> USP produces low surface area powders, undesirable for catalysis. The technique described herein provides a general aerosol route to high surface area materials. We find that the highly porous MoS<sub>2</sub> so produced has exceptionally high HDS activity.

Porous MoS<sub>2</sub> was prepared by USP using colloidal silica as a sacrificial template, with (NH<sub>4</sub>)<sub>2</sub>MoS<sub>4</sub><sup>8</sup> as a MoS<sub>2</sub> precursor. The precursor solution is ultrasonically nebulized into microdroplets,<sup>9</sup> which are carried by a gas flow into a furnace where solvent evaporation and precursor decomposition occurs, producing a SiO<sub>2</sub>/MoS<sub>2</sub> composite. Material is collected and treated with HF, leaving a MoS<sub>2</sub> network, whose porosity and surface area can be controlled by changing the size and concentration of the template.

For comparison, conventional MoS<sub>2</sub> and nontemplated USP MoS<sub>2</sub> were prepared by thermal decomposition of (NH<sub>4</sub>)<sub>2</sub>MoS<sub>4</sub>. SEMs<sup>10</sup> of the conventional layered, platelike MoS<sub>2</sub> (Figure 1A) contrast dramatically with the porous networks of the templated USP MoS<sub>2</sub> (Figure 1C,D). TEMs of the USP product before and after leaching are shown in Figure 1E,F. Before leaching, both colloidal SiO<sub>2</sub> and MoS<sub>2</sub> can be seen, and the SiO<sub>2</sub> and MoS<sub>2</sub> are woven within each other. This suggests MoS<sub>2</sub> formation occurs within the crevices created as the SiO<sub>2</sub> spheres compact during solvent evaporation. After HF leaching, the MoS<sub>2</sub> is network-like, but retains the lattice fringes of the MoS<sub>2</sub> interlayer spacings (0.42 ± 0.01 nm, Figure 1F), similar to that of conventional MoS<sub>2</sub>.

The XRD patterns of heat-treated USP and conventional MoS<sub>2</sub> samples showed four broad peaks with *d* spacings of 6.4, 2.7, 1.6, and 1.2 Å, corresponding to the {002}, {100}, {103}, and {110} reflections, respectively, of poorly crystalline, nanostructured 2H-MoS<sub>2</sub>.<sup>10</sup> The average *c*-stacking height, calculated from the {002} reflection, was 37 Å for conventional MoS<sub>2</sub> and 35 Å for nontemplated USP MoS<sub>2</sub>, but only 25 Å for 20 nm silica-templated MoS<sub>2</sub>. When larger diameter SiO<sub>2</sub> templates are used, the *c*-stacking increases to that of conventional MoS<sub>2</sub>.

The electronic states of Mo and S in the heat-treated USP MoS<sub>2</sub> samples were determined by X-ray photoelectron spectroscopy (XPS), which showed spin-coupled Mo(3d<sub>5/2</sub>, 3d<sub>3/2</sub>) and S(2p<sub>3/2</sub>, 2p<sub>1/2</sub>) doublets at the binding energies of conventional MoS<sub>2</sub>.<sup>10</sup> Analysis of the Mo(3d) and S(2p) peak intensities gave a S/Mo atomic ratio slightly less than 2 for all samples.

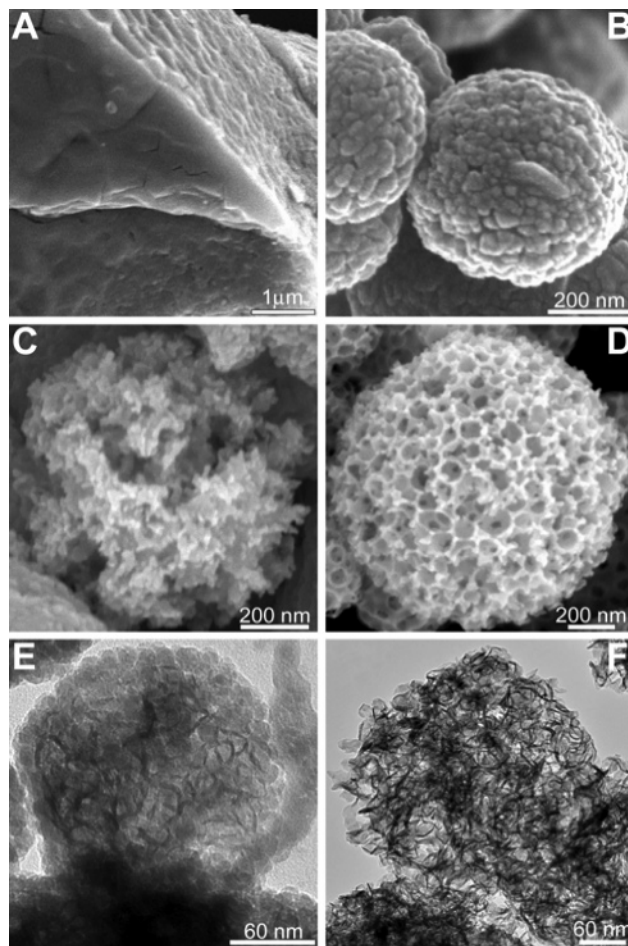


**Figure 1.** Electron micrographs of conventional and USP-derived MoS<sub>2</sub>. (A) SEM of conventional MoS<sub>2</sub>. (B) SEM of USP MoS<sub>2</sub> without templating material. (C) SEM of 20 nm silica-templated USP MoS<sub>2</sub>, after leaching of the colloidal silica. (D) SEM of 80 nm silica-templated USP MoS<sub>2</sub>, after leaching of the colloidal silica. (E) TEM of USP SiO<sub>2</sub>/MoS<sub>2</sub> composite (prior to leaching, 20 nm SiO<sub>2</sub> template). (F) TEM of 20 nm silica-templated USP MoS<sub>2</sub>, after leaching of the colloidal silica.

Figure 2 shows complete N<sub>2</sub> adsorption–desorption isotherms for several USP preparations and, for comparison, conventional MoS<sub>2</sub> with total surface areas, determined by BET analysis.<sup>10</sup> Without templating, low surface area MoS<sub>2</sub> is obtained (20–40 m<sup>2</sup>/g) by USP, which is comparable to conventional preparations; however, with templating, the surface area can be controlled and substantially enhanced. In fact, when 20 nm SiO<sub>2</sub> is used as a template, the USP MoS<sub>2</sub> has a surface area comparable to that of a commercial catalyst support (e.g., Crosfield 465 1:20 Co–Mo on  $\gamma$ -alumina is 210 m<sup>2</sup>/g), but the MoS<sub>2</sub> itself is acting as the dispersion phase rather than a separate support material. The USP products display no plateau region in the N<sub>2</sub> isotherms; this, in

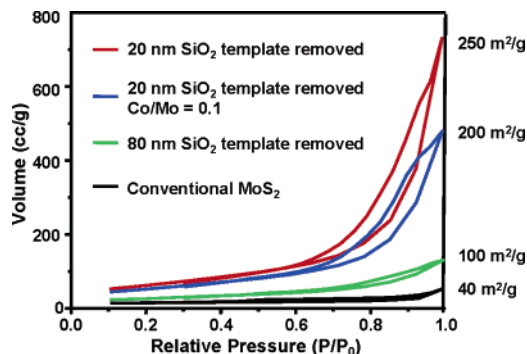


**Figure 2.** N<sub>2</sub> adsorption–desorption isotherms for various catalysts and corresponding BET surface areas.

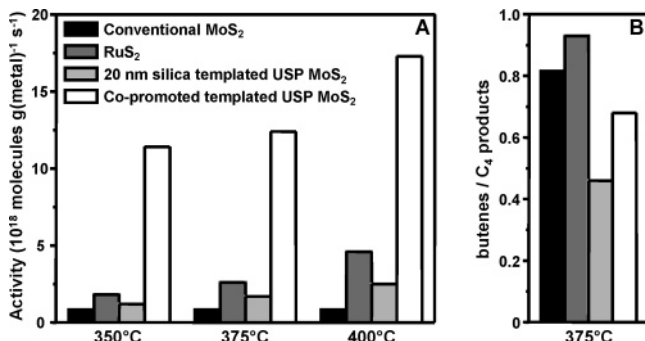


**Figure 3.** (A) Catalytic activities of various catalysts for thiophene HDS as a function of temperature after 12 h of catalysis, which is necessary to reach steady-state activity for these catalysts; initial rates show larger temperature differences, as expected. (B) Fraction of butenes in C<sub>4</sub> hydrocarbon product mixture observed during thiophene HDS at 375 °C.

conjunction with the high surface area, is characteristic of both micro- and macroporosity.<sup>11</sup> Such a combination is potentially ideal for the HDS of fuel residua.

The catalytic activity of thiophene HDS for the heat-treated USP MoS<sub>2</sub> samples was examined with a single-pass microreactor at 1 atm (Figure 3).<sup>12</sup> Of the USP samples, the 20 nm silica-templated MoS<sub>2</sub> obtained the greatest HDS activities.<sup>13</sup> Additionally, cobalt-promoted USP MoS<sub>2</sub> samples were prepared by salt impregnation;<sup>14</sup> maximum activity was achieved with a Co/Mo ratio of 0.1. At higher Co/Mo ratios, a decrease in catalytic activity and the formation of a separate cobalt sulfide phase, Co<sub>9</sub>S<sub>8</sub>, were observed. These samples were compared to conventional catalysts of MoS<sub>2</sub> and RuS<sub>2</sub> (60 m<sup>2</sup>/g); RuS<sub>2</sub> is the most intrinsically active metal sulfide for HDS, but too expensive to be used industrially.<sup>15</sup> The results are shown in Figure 3A; catalyst activities are reported on a per gram of metal basis because HDS activity of MoS<sub>2</sub> does not scale with total surface area due to the different reactivity of edge and basal planes and Co promotion of edge sites.<sup>16</sup> The nonpromoted templated USP MoS<sub>2</sub> was more active than conventional MoS<sub>2</sub> and is attributed to the enhanced dispersion of the HDS active phase achieved by this technique. Upon cobalt incorporation, the activity of the USP MoS<sub>2</sub> is well above that even of RuS<sub>2</sub>.

Figure 3B shows the mole fraction of butenes in the total product mixture of C<sub>4</sub> hydrocarbons at 375 °C. No butadiene or tetrahydrothiophene were observed. The nonpromoted USP MoS<sub>2</sub> had an increased percent butane compared to that of conventional MoS<sub>2</sub>, reflecting the higher activity of USP MoS<sub>2</sub>. The selectivity for butenes increased upon cobalt incorporation, as expected.<sup>17</sup>

In summary, a high surface area MoS<sub>2</sub> network can be synthesized by USP by using a sacrificial colloidal silica template. The resulting highly porous MoS<sub>2</sub> network has higher thiophene HDS activity than that of conventional MoS<sub>2</sub> and when promoted with cobalt, higher even than RuS<sub>2</sub>. By controlling the template size and concentration, a unique micro- and macroporous form of MoS<sub>2</sub> can be prepared that may provide enhanced diffusion rates and decreased residence times, requirements for improved HDS catalysts.

**Acknowledgment.** We thank Dr. Y. Didenko for helpful advice. These studies were supported by the NSF (CHE0315494). Microscopic analysis, XRD, and XPS were carried out in the Center for Microanalysis of Materials, University of Illinois, which is partially supported by the U.S. Department of Energy under Grant DEFG02-91-ER45439.

**Supporting Information Available:** Additional electron micrographs, XPS spectra, and XRD data. This material is available free of charge via the Internet at <http://pubs.acs.org>.

## References

- (1) (a) Furimsky, E. *Appl. Catal. A* **1998**, *171*, 177–206. (b) Grange, P. *Catal. Rev. Sci. Eng.* **1980**, *21*, 135–181.
- (2) *Federal Register*, August 4 2002, 65 (151), 48057–48105.
- (3) (a) Raseev, S. *Thermal and Catalytic Processes in Petroleum Refining*; Suci, G. D., Ed.; Marcel Dekker: New York, 2003. (b) Speight, J. G. *The Desulfurization of Heavy Oils and Residua*, 2nd ed.; Heinemann, H., Ed.; Chemical Industries; Marcel Dekker: New York, 2000.
- (4) (a) Dhas, N. R.; Ekhtiarzadeh, A.; Suslick, K. S. *J. Am. Chem. Soc.* **2001**, *123*, 8310–8316. (b) Zdrzil, M. *Catal. Today* **1988**, *3*, 269–361.
- (5) (a) Mdeleni, M. M.; Hyeon, T.; Suslick, K. S. *J. Am. Chem. Soc.* **1998**, *120*, 6189–6190. (b) Afanasiev, P.; Xia, G. F.; Gilles, B.; Jouguet, B.; Lacroix, M. *Chem. Mater.* **1999**, *11*, 3216–3219.
- (6) (a) Messing, G. L.; Zhang, S. C.; Jayanthi G. V. *J. Am. Ceram. Soc.* **1993**, *76*, 2707–2726. (b) Patil, P. S. *Mater. Chem. Phys.* **1999**, *59*, 185–198. (c) Kodas, T. T.; Hampden-Smith, M. *Aerosol Processing of Materials*; Wiley-VCH: New York, 1999. (d) Okuyama, K.; Lenggoro, I. W. *Chem. Eng. Sci.* **2003**, *58*, 537–547. (e) Tsai, S. C.; Long, Y. L.; Tsai, C. S.; Yang, C. C.; Chiu, W. Y.; Lin, H. M. *J. Mater. Sci.* **2004**, *39*, 3647–3657.
- (7) (a) Iskandar, F.; Mikrajuddin; Okuyama, K. *Nano Lett.* **2002**, *2*, 389–392. (b) Xia, B.; Lenggoro, W.; Okuyama, K. *Adv. Mater.* **2001**, *13*, 1579–1582. (c) Iskandar, F.; Mikrajuddin; Okuyama, K. *Nano Lett.* **2001**, *1*, 231–234.
- (8) (a) Berntsen, N.; Gutjahr, T.; Loeffler, L.; Gomm, J. R.; Seshadri, R.; Tremel, W. *Chem. Mater.* **2003**, *15*, 4498–4502. (b) Vasudevan, P. T.; Zhang, F. *Appl. Catal. A* **1994**, *112*, 161–173.
- (9) In a typical synthesis, a 0.04 M (NH<sub>4</sub>)<sub>2</sub>MoS<sub>4</sub> aq. solution containing colloidal SiO<sub>2</sub> (e.g., 5-fold molar excess 20 nm LUDOX HS-40 or 80 nm SNOWTEX-ZL) was nebulized using a Sunbeam Ultrasonic Humidifier (2.7 MHz), carried in an Ar flow (2 cfh) through a furnace (700 °C) and collected in bubblers. No (NH<sub>4</sub>)<sub>2</sub>MoS<sub>4</sub> decomposition is observed in the atomization cell. SiO<sub>2</sub> was leached with 10% HF in C<sub>2</sub>H<sub>5</sub>OH for 24 h, confirmed by e.a. and EDS. Samples were treated with 5% H<sub>2</sub>S/45% H<sub>2</sub>/50% He (30 cm<sup>3</sup>/min) at 450 °C for 12 h. E.A. shows nearly stoichiometric MoS<sub>2</sub> with trace (<2 wt %) carbon and oxygen.
- (10) Hitachi S-4700 SEM with Oxford INCA EDS; Philips CM-12 TEM; Rigaku D-MAX diffractometer; Physical Electronics PHI 5400 XPS; Quantachrome Instruments Nova 2200e Surface Area and Pore Analyzer.
- (11) Gregg, S. J.; Sing, K. S. *Adsorption, Surface Area, and Porosity*; Academic Press: New York, 1967.
- (12) Thiophene vapor at 56.25 Torr in H<sub>2</sub> flow (27.5 cm<sup>3</sup>(STP)/min). Analysis by GC–MS with a 30 m carbon PLOT column.
- (13) MoS<sub>2</sub> prepared by USP without a template and with 80 nm silica template (after leaching of the silica) shows thiophene HDS activities at 350 °C of 0.4 and 1.6 × 10<sup>18</sup> molecules g(metal)<sup>-1</sup> s<sup>-1</sup>, respectively.
- (14) Co(NO<sub>3</sub>)<sub>2</sub>·6H<sub>2</sub>O dissolved in acetone was added in the appropriate stoichiometry to the solid catalyst, which was then dried and heat treated.
- (15) Pecoraro, T. A.; Chianelli, R. R. *J. Catal.* **1981**, *67*, 430–445.
- (16) (a) Tauster, S. J.; Pecoraro, T. A.; Chianelli, R. R. *J. Catal.* **1980**, *63*, 515–519. (b) Chianelli, R. R.; Daage, M. *J. Catal.* **1994**, *149*, 414–427. (c) Topsøe, H. *J. Catal.* **2003**, *216*, 155–164. (c) Inamura, K.; Prins, R. *J. Catal.* **1994**, *147*, 515–524.
- (17) Hatanaka, S.; Yamada, M.; Sadakane, O. *Ind. Eng. Chem. Res.* **1997**, *36*, 5110–5117.

JA051654G